科技部補助專題研究計畫成果報告
期末報告

荷重型高骨形成性生物陶瓷複合材料研發(第3年)

計 畫 類 別 ： 個別型計畫
計 畫 編 號 ： MOST 104-2221-E-040-004-MY3
執 行 期 間 ： 106年08月01日至107年07月31日
執 行 單 位 ： 中山醫學大學口腔科學研究所

計 畫 主 持 人 ： 丁信智

計畫參與人員： 博士後研究-博士後研究：朱殷弘

報 告 附 件 ： 出席國際學術會議心得報告

中 華 民 國 107 年 07 月 26 日

中 文 摘 要 ： 氧化鋯（ZrO2）陶瓷因其在醫療應用中的優異機械性能和體內化學穩定性而備受關注。然而，該材料對細胞和組織的親和力差，這對於骨植入物應用而言，需加以克服。因此，需要進一步開發ZrO2基的高效能材料。矽酸鈣（CaSi）的材料由於其高成骨性，而越來越受重視，用於骨移植替代物。本計畫致力於設計新的ZrO2基植體，並添加CaSi以增強此結構植入物陶瓷的成骨性。評估CaSi對ZrO2基骨植體的相組成，長期體外降解性和骨形成性的影響。實驗結果顯示CaSi添加劑不影響ZrO2的四方-單斜相變。含5和10 wt% CaSi的複合材料具有與ZrO2相比擬的三點彎曲強度和雙軸強度值，而過量的CaSi導致強度降低。然而，15和20 wt% CaSi的複合材料的三點彎曲強度在皮質骨彎曲強度範圍內。有趣的是，複合植入物的彎曲模量隨著CaSi含量的增加而降低。對於體外降解，除了20wt% CaSi植入物的輕微重量損失（小於1%）之外，隨著浸泡時間的增加，所有骨植入物都沒有明顯變化。正如所料，較高的CaSi植入物明顯增強了ZrO2植入物的生物學功能。結論是CaSi-ZrO2複合植體為ZrO2用於承重骨植入物提供了一種很有前途的替代方案。

中 文 關 鍵 詞 ： 氧化鋯、矽酸鈣、複合植體，荷重應用，骨形成性

英 文 摘 要 ： Zirconia (ZrO2) ceramic has attracted much attention because of its superior mechanical properties and chemical stability in vivo for medical applications. However, this material has a poor affinity to cells and tissues, which needs to be overcome for bone implant applications. Thus, further research is required to develop a high efficacy ZrO2-based material candidate. Calcium silicate (CaSi)-based materials have gained increasing interest for use as bone graft substitutes because of their high osteogenesis. Efforts have been oriented toward the design of novel ZrO2-based systems where CaSi was added to enhance the osteogenesis of the structural implant ceramics. The effect of CaSi on the phase composition, long-term in vitro degradation, and osteogenesis of the ZrO2-based osteo-implants was evaluated. The experimental results revealed that the CaSi additive did not affect the tetragonal-monoclinic phase transformation of ZrO2. The 5 and 10 wt% CaSi-containing composites had three-point bending strength and biaxial strength values comparable to those of the ZrO2 control, whereas excessive CaSi resulted in the decreased strength. However, the three-point bending strength of 15 and 20 wt% CaSi-containing composites was within the reported bending strength for cortical bone. Interestingly, the bending modulus of the composite implants decreased with the increasing CaSi content. For the in vitro degradation, there were no obvious changes for all osteo-implants with the increasing soaking time, except the slight weight loss (less than 1%) of the 20 wt% CaSi implant. As expected, the higher CaSi implants appreciably

enhanced the biological functions of the ZrO2 implant. It is concluded that the CaSi-ZrO2 composite osteo-implants offered a promising alternative to ZrO2 for load-bearing bone implant application.

英文關鍵詞：Zirconia, Calcium silicate, Composite implants, Load-bearing application, Osteogenesis

1. 中文摘要

氧化鋯（ZrO_2）陶瓷因其在醫療應用中的優異機械性能和體內化學穩定性而備受關注。然而，該材料對細胞和組織的親和力差，這對於骨植入物應用而言，需加以克服。因此，需要進一步開發 ZrO_2 基的高效能材料。矽酸鈣（CaSi）的材料由於其高成骨性，而越來越受重視，用於骨移植替代物。本計畫致力於設計新的 ZrO_2 基植體，並添加 CaSi 以增強此結構植入物陶瓷的成骨性。評估 CaSi 對 ZrO_2 基骨植體的相組成，長期體外降解性和骨形成性的影響。實驗結果顯示 CaSi 添加劑不影響 ZrO_2 的四方-單斜相變。含 5 和 10 wt% CaSi 的複合材料具有與 ZrO_2 相比擬的三點彎曲強度和雙軸強度值，而過量的 CaSi 導致強度降低。然而，15 和 20 wt% CaSi 的複合材料的三點彎曲強度在皮質骨彎曲強度範圍內。有趣的是，複合植入物的彎曲模量隨著 CaSi 含量的增加而降低。對於體外降解，除了 20wt% CaSi 植入物的輕微重量損失（小於 1%）之外，隨著浸泡時間的增加，所有骨植入物都沒有明顯變化。正如所料，較高的 CaSi 植入物明顯增強了 ZrO_2 植入物的生物學功能。結論是 CaSi-ZrO_2 複合植體為 ZrO_2 用於承重骨植入物提供了一種很有前途的替代方案。

關鍵詞：氧化鋯、矽酸鈣、複合植體，荷重應用，骨形成性

2. 英文摘要

Zirconia (ZrO_2) ceramic has attracted much attention because of its superior mechanical properties and chemical stability *in vivo* for medical applications. However, this material has a poor affinity to cells and tissues, which needs to be overcome for bone implant applications. Thus, further research is required to develop a high efficacy ZrO_2-based material candidate. Calcium silicate (CaSi)-based materials have gained increasing interest for use as bone graft substitutes because of their high osteogenesis. Efforts have been oriented toward the design of novel ZrO_2-based systems where CaSi was added to enhance the osteogenesis of the structural implant ceramics. The effect of CaSi on the phase composition, long-term *in vitro* degradation, and osteogenesis of the ZrO_2-based osteo-implants was evaluated. The experimental results revealed that the CaSi additive did not affect the tetragonal-monoclinic phase transformation of ZrO_2. The 5 and 10 wt% CaSi-containing composites had three-point bending strength and biaxial strength values comparable to those of the ZrO_2 control, whereas excessive CaSi resulted in the decreased strength. However, the three-point bending strength of 15 and 20 wt% CaSi-containing composites was within the reported bending strength for cortical bone. Interestingly, the bending modulus of the composite implants decreased with the

increasing CaSi content. For the *in vitro* degradation, there were no obvious changes for all osteo-implants with the increasing soaking time, except the slight weight loss (less than 1%) of the 20 wt% CaSi implant. As expected, the higher CaSi implants appreciably enhanced the biological functions of the ZrO_2 implant. It is concluded that the CaSi-ZrO_2 composite osteo-implants offered a promising alternative to ZrO_2 for load-bearing bone implant application.

Keywords: Zirconia, Calcium silicate, Composite implants, Load-bearing application, Osteogenesis

3. Introduction and purpose

Titanium and titanium alloys have been used as implant materials owing to its corrosion resistance, low density and superior mechanical properties, but they exhibits poor bioactive properties and fails to firmly bind to the bone tissues [1–3]. In addition, the problems like gingival tarnishing and peri-implantitis have been reported in the dentistry [4,5]. Ceramic materials have been considered as alternatives to metals for implant applications such as total hip and knee replacements and dental restorations [6−8]. Among the ceramics, zirconia (ZrO_2) has been one of the most important ceramic materials and offers the highest fracture toughness due to transformation toughening [9–12], in addition to good abrasion resistance, chemical stability *in vivo*. Moreover, an *in vivo* experimental study has reported that ZrO_2 implants have no negative effects on soft and hard tissues as well as the similar osteointegration to titanium implants [13]. Nevertheless, this material has no direct bone bonding properties, only showing a morphological fixation with the surrounding tissues alone [14,15]. As an ideal implant material, to pursue the high biocompatibility is still a concerned theme, although commercial ZrO_2 systems are available today. A number of articles have been reported regarding methods for endowing zirconia surface with biological activity. Pelaez-Vargas *et al.* [16] modified the surfaces of ZrO_2 implants with micropatterned silica to enhance guided tissue regeneration on ceramic dental implants. On the other hand, the addition of bioactive materials to a zirconia matrix is another approach to solve the problem of bioinertness in zirconia-based implants [19–20]. For examples, the Yamashita' group doped a small amount of hydroxyapatite to Yttria-stabilized tetragonal zirconia polycrystal (Y-TZP) to produce a composite biomaterial with a high bioactivity as well as sufficient mechanical strength and fracture toughness for a heavy load [18]. Marchi *et al.* [19] took advantage of the bioactivity of TiO_2 ceramics to enhance the biological properties of ZrO_2.

Calcium silicate-based bone graft substitutes, such as bioactive glass [14,21] and

calcium silicate ceramic [22] have been developed for hard tissue applications. The *in vitro* cell culture studies have shown that the calcium silicate-based materials can expedite the osteogenesis of the human bone mesenchymal stem cell [23] and human pulp cell [24]. More importantly, newly formed bone tissue can grow on the surface of the calcium silicate-based materials, along with the deposition of a bone-like apatite layer at the tissue/material interface [25]. Hence, calcium silicate can be used as reinforcing phase for its higher osteogenesis.

Aforementioned, further research is required to develop an effective and competitive zirconia-based material candidate as a clinical alternative to titanium implants for load-bearing applications. An ideal implant material would have the enough mechanical characteristics and excellent biological properties to match the properties of bone defect. To improve the osteogenesis of the dental zirconia ceramics the incorporation of the calcium silicate (CaSi) into zirconia was developed. The effect of CaSi on the mechanical properties, *in vitro* degradation, and *in vitro* osteogenic activity of the composite osteo-implants was evaluated.

4. Materials and methods

4.1. Preparation of composites

The details of the procedure for the preparation of the sol-gel-derived calcium silicate powder as a starting material have been described elsewhere [22]. Reagent-grade tetraethyl orthosilicate ($Si(OC_2H_5)_4$) (Sigma–Aldrich, St. Louis, MO, USA) and calcium nitrate ($Ca(NO_3)_2{\cdot}4H_2O$) (Showa, Tokyo, Japan) were used as precursors for SiO_2 and CaO, respectively. Nitric acid was used as the catalyst, and ethanol was used as the solvent. The general sol-gel procedure, including hydrolysis and aging, was used here. Briefly, $Si(OC_2H_5)_4$, was hydrolyzed by the sequential addition of 2 M HNO_3 and absolute ethanol, with 1 h of stirring after each addition. $Ca(NO_3)_2{\cdot}4H_2O$ was added to the $Si(OC_2H_5)_4$ solution in an equimolar ratio, and the mixture was stirred for an additional 1 h. The molar ratio of (HNO_3 + H_2O)–$Si(OC_2H_5)_4$–ethanol was 10:1:10. The mixture was sealed and aged at 60 °C for 1 day before vaporization of the solvent in an oven at 120 °C. This dried calcium silicate powders was added to the submicro Y_2O_3-stabilized ZrO_2 powder (Sigma-Aldrich) at 5, 10, 15, and 20 wt% using a Thinky ARE-250 defoaming mixer (Tokyo, Japan) at 1,000 rpm for 15 min and then ball-milled for 5 h in ethyl alcohol by a Retsch S 100 centrifugal ball mill (Hann, Germany) and dried in an oven at 120 °C overnight. The sample code “ZCS10” represents the mixture containing 10 wt% CaSi, as listed in Table 1. The mixtures were compacted into 24 mm × 4 mm × 4 mm rectangular bars or 15 mm diameter cylindrical pellets by uniaxial pressing at 100 MPa. After this, the green bodies were sintered at 1350 °C at a heating rate of 10 ℃/min

for 2 h using a high-temperature furnace, then furnace-cooled to room temperature. Each sample was polished with a 1 μm diamond paste.

4.2. Phase composition and morphology

Phase analysis was performed using an X-ray diffractometry instrument (XRD; Bruker D8 SSS, Karlsruhe, Germany) with Ni-filtered Cukα radiation operating at 40 kV, 100 mA and a scanning speed of 0.5 °/min. A Fourier transform infrared spectroscopy apparatus (FTIR; Bruker Vertex 80v, Ettlingen, Germany) in reflection absorption mode with a spectral resolution of 1 cm^{-1} in a wavenumber range of 400−4000 cm^{-1} was used to characterize the various functional groups. The microstructure was observed by field-emission scanning electron microscopy (SEM; JEOL JSM-7800F, Tokyo, Japan) on the mirror polished surface. The samples were coated with gold using a JFC-1600 (JEOL) coater and examined by SEM operating in the lower secondary electron image mode at 3 kV accelerating voltage.

4.3. Mechanical properties

4.3.1 Three-point bending strength

Three-point bending test was conducted, according to the ISO 6872:2008 standards [26], on a static mechanical testing machine AG-1000E (Shimadzu, Kyoto, Japan) with a 10 kN load cell at a crosshead speed of 1 mm/min. After sintering at 1350 °C, the final dimensions of rectangular specimens were about 18 mm × 3 mm × 3 mm. Prior to the bending strength test, the dimensions of the specimens were measured with a digital micrometer (Absolute Digimatic Caliper, Mitutoyo, Tokyo, Japan) to an accuracy of 0.01 mm. Span length was 16 mm. With the bending of samples, ultimate bending strength (σ_b) and Young's bending modulus (E_b) were calculated as follows [27]:

$$\sigma_b = \frac{3F_{\max}L}{2wt^2} \quad \text{and} \quad E_b = \frac{L^3}{4wt^3}\frac{\Delta F}{\Delta l}$$

where F_{max} is the maximum load (N), L the support span (mm), w and t are width (mm) and thickness (mm) of specimen, respectively, $\Delta F/\Delta l$ the slope of the initial linear elastic portion of the load–deflection curve (N/mm). The data provided for each group were the mean of twenty independent measurements.

4.3.2. Biaxial flexural strength

Each cylindrical specimen was placed centrally on three hardened steel balls (with the diameter of 3 mm, positioned 120° apart on a support circle with a diameter of 10 mm. The polished surface of the specimen was the tension side while the unpolished surface was loaded with a flat punch (1.2 mm in diameter). The biaxial flexural strength was

obtained using an AG-1000E where the load was applied at a constant speed of 1 mm/min until fracture occurred. The load that led to the initial separation of specimens was obtained in Newton (N) and converted to MPa using the following equation, according to ISO 6872 [26]:

$$S = -0.2387P(X-Y)/d^2$$

where '*S*' is the maximum center tensile stress (MPa), '*P*' is the total load causing fracture (N);

$$X = (1+\nu)\mathrm{In}(r_2/r_3)^2+[(1-\nu)/2](r_2/r_3)^2$$

$$Y = (1+\nu)[1+\mathrm{In}(r_1/r_3)^2]+(1-\nu)(r_1/r_3)^2$$

v: Poisson ratio. If the value for the ceramic concerned is not known, a Poisson's ratio = 0.25 is used; r_1: radius of support circle (mm); r_2: radius of loaded area (mm); r_3: radius of specimen (mm); *d*: specimen thickness at fracture origin (mm).

4.3.3. Weibull analysis

To understand the level of the structural reliability of the materials, a Weibull analysis was commonly used to analyze historical failure data and produce failure distributions. The twenty measurements of failure strength from each group were ranked in order from the weakest to the strongest. The description of the Weibull distribution was given by the formula:

$$F(\sigma) = 1- \exp [-(\sigma/\sigma_o)m]$$

where $F(\sigma)$ is the failure probability (defined by the relation of $F(\sigma) = i/(N+1)$, in which *i* is the rank order of the compressive strength and *N* is the number of specimens), σ is the strength at a given $F(\sigma)$, σ_o is the characteristic strength (scale parameter) at the fracture probability of 62%, and m is the Weibull modulus (shape parameter) [28].

4.4. In vitro degradation

The simulated body fluid (SBF) solution, an extracellular solution with an ionic composition similar to that of human blood plasma, was used as the supporting solution for the *in vitro* degradation tests. In order to simulate the constant circulation of physiological fluids in the body, continuous exchange (dynamic condition) of SBF may be a more effective assay which makes more precise predictions of the degradation than a static assay (the lack of SBF exchange). Exchange of solution could maintain the ionic concentration and pH of SBF almost constant and close to plasma, which provides a fresh solution [27]. It consisted of 7.9949 g of NaCl, 0.3528 g of $NaHCO_3$, 0.2235 g of KCl, 0.147 g of K_2HPO_4, 0.305 g of $MgCl_2 \cdot 6H_2O$, 0.2775 g of $CaCl_2$, and 0.071 g of Na_2SO_4 in 1000 mL of distilled H_2O and was buffered to pH 7.4 with hydrochloric acid (HCl; Merck, Darmstadt, Germany) and trishydroxymethyl amino methane (Tris,

$CH_2OH)_3CNH_2$; Sigma–Aldrich). All used chemicals were of reagent grade and used as obtained. After soaking for specific time duration (1, 3, 6, and 12 months), twenty specimens were removed from the vials to evaluate biaxial strength. The other specimens were dried in an oven at 60 ℃ for the analyses of weight loss, phase composition, and morphology. For the measurement of weight loss, the dried specimens were weighed until reaching a constant weight before (day 0) and after immersion using a four-digit balance (AE 240S, Mettler-Toledo AG, Greifensee, Switzerland). Twelve repeated specimens were examined for each of the materials investigated at each time point.

4.5. In vitro osteogenic activity

4.5.1. Cell culture

MG63 human osteoblast-like cells (BCRC 60279; Hsinchu, Taiwan) were used to evaluate cell behavior. They were suspended in Dulbecco's modified Eagle medium (DMEM; Gibco, Langley, OK) containing 10% fetal bovine serum (FBS) (Gibco) and 1% penicillin (10,000 U/mL)/streptomycin (10,000 μg/mL) solution (Gibco) in 5% CO_2 at 37 °C. Prior to cell incubation, the samples were sterilized by soaking in a 75% ethanol solution and exposure to ultraviolet (UV) light for 2 h. MG63 cell suspensions at a density of 10^4 cells/mL were seeded over each of the samples.

4.5.2. Cell attachment and proliferation

To assess attachment, cells were cultured for 6 h, 12 h, and 1 day. Proliferation was assessed at days 3 and 7. After the established incubation period, cell viability was examined using the MTT (3-(4,5-dimethylthiazol-2-yl)-2,5-diphenyltetrazolium bromide; Sigma−Aldrich) assay, in which tetrazolium salt is reduced to formazan crystals by the mitochondrial dehydrogenase of living cells. Briefly, 4 h before the end of the incubation period, 200 μL of 0.5 mg/mL MTT solution in DMEM containing 1% penicillin/streptomycin and 200 μL of dimethylsulfoxide (Sigma−Aldrich) were added to each well. The plates were then shaken until the formazan crystals had dissolved, and 100 μL of the solution from each well was transferred to a 96-well tissue-culture plate. Plates were read in a Sunrise microplate reader (Tecan, Salzburg, Austria) at 570 nm, with a reference wavelength of 690 nm. The results were reported in terms of absorbance. The results were obtained in six independent measurements.

*4.5.3. A*lkaline *phosphatase activity*

To evaluate the effect of CaSi content on early cell differentiation, the alkaline phosphatase (ALP) activity assay was carried out using a TRACP & ALP assay kit (Takara, Shiga, Japan) according to the manufacture's instructions. ALP catalyzes the

hydrolysis of the colorless organic phosphate ester substrate, *p*-nitrophenyl phosphate (pNPP), to *p*-nitrophenol, a yellow product, and phosphate. To perform the assay, after 7 and 14 days of incubation, the cells were washed with physiological saline (150 mM NaCl) and lysed in 50 µL of lysis buffer (1% NP40 in 150 mM NaCl). For measurement purposes, 50 µL of the substrate solution (20 mM Tris–HCl, 1 mM $MgCl_2$, 12.5 mM pNPP, pH = 9.5) was added to each well and allowed to react at 37 °C for 30 min in the dark. The reaction was stopped by the addition of 50 µL of 0.9 M NaOH and read at 405 nm using a Sunrise microplate reader. Three dependent measurements were made.

4.5.4. Calcium quantification

The mineralized matrix synthesis was analyzed using an Alizarin Red S staining method, which identifies calcium deposits. After culture for 7 and 14 days, the cells were washed with PBS and fixed in 4% paraformaldehyde (Sigma–Aldrich) for 10 min at 4 ºC. This was followed by staining for 10 min in 0.5% Alizarin Red S (Sigma–Aldrich) in PBS at room temperature. Cells were completely washed with PBS and then observed using an optical microscope (BH2-UMA; Olympus, Tokyo, Japan). To quantify matrix mineralization, the calcium mineral precipitate was destained by 10% cetylpyridinium chloride (Sigma–Aldrich) in PBS for 30 min at room temperature. The absorbance of Alizarin Red S extracts was measured at 562 nm using a Sunrise microplate reader. Mean absorbance values were obtained from three independent experiments. Three measurements were made.

4.6. Statistical analysis

One-way analysis of variance (ANOVA) was used to evaluate the significant differences between the means in the measurement data. Scheffe's multiple comparison testing is used to determine the significance of the standard deviations in the measurement data of each specimen for different experimental conditions. In all cases, the results are considered statistically different at *p*-value of less than 0.05.

5. Results

5.1. Phase composition and microstructure

XRD patterns of initial calcium silicate powder, as-received ZrO_2 powder, and the sintered bodies are shown in Fig. 1. From the broad nature of the peaks, the initial CaSi powder revealed the amorphous phase because of unsintering (Fig 1a). The as-received ZrO_2 powder had tetragonal zirconia (t-ZrO_2) phases (Fig. 1b) mainly consisting of 2θ = 30.2°, 35.0°, 50.1°, and 59.7° attributed to (101), (110), (112), and (211) crystal faces [12], along with small amounts of monoclinic zirconia (m-ZrO_2) phased at 2θ = 28.2°

(−111) and 31.5° (111). In addition, the (200), (220), and (−203) monoclinic crystal faces overlapped with the (110), (112), and (211) tetragonal phases, respectively [12]. After sintering, in addition to the increased peak intensity of t-ZrO_2 due to the elevated temperature, no new peaks were observed for the ZrO_2 control in contrast, when 20 wt% CaSi powder was added to the ZrO_2 powder, the sintered composite mainly exhibited t-ZrO_2 phase, along with possibly appearing the $CaZrO_3$ phase at 2θ = 31.7° [28] and $CaSiO_3$ at 30.1° [29] (overlapped with t-ZrO_2), and other undetected calcium zirconium silicate phase [30].

The surface features of the osteo-implants were further analyzed by FTIR-DRIFT technique (Fig. 2), which revealed different functional groups on the surface of the samples with and without CaSi component. As expected, all samples revealed Zr–O bond vibration at about 610 cm^{-1} [31]. The band at 2370 cm^{-1} can be attributed to C–O stretching [32]. When CaSi was added to the ZrO_2, the bands at about 700 cm^{-1} were ascribed to $CaSiO_3$ [29], along with new band between 1550 and 1650 cm^{-1}. A mall peak observed at around 960 cm^{-1} corresponded to the Si–O–Zr bonds [33], suggesting the formation of a zirconia and silica phase.

Broad-face SEM micrographs of the specimens are shown in Fig. 3. The ZrO_2 control (ZCS0) appeared rather dense looking without pores. It seems that the low amount (5 and 10 wt%) of the CaSi additive did not induce the change of the microstructure on the control surfaces. Contrary to the findings, 15 and 20 wt% CaSi would result in the formation of the micropores.

5.2. Mechanical properties

5.2.1. Three-point bending strength and modulus

Table 1 lists the relationships between the three-point bending and modulus for the implants, along with letter codes from Scheffe's *post hoc* multiple comparison. The samples showed non-monotonous changes in strength and a significant difference ($p < 0.05$) among the osteo-implants was found. Interestingly, the 5 and 10 wt% CaSi-containing groups had a three-point bending strength value comparable to the strength of the control without CaSi (183 MPa). After the addition of 15 and 20 wt% CaSi, the three-point bending strength of the composite implants decreased to 162 and 132 MPa, respectively, which were significantly lower values than the ZrO_2 control. The values of the mean elastic moduli were in the range of 24.5 to 19.0 GPa, indicating the trend to decrease with the increasing CaSi content, along with a significant difference ($p < 0.05$).

5.2.2. Biaxial flexural strength

There were significant differences ($p < 0.05$) in biaxial flexural strength among the

samples, as presented in Table 1. The composite implant containing 5 wt% CaSi had a biaxial strength value of 354 MPa on average, slightly higher than the control (335 MPa). The addition of 10, 15, and 20 wt% CaSi to the ZrO_2 implant led to the biaxial strength of 324, 223, and 164 MPa, respectively.

5.2.3. Weibull analysis

Fig. 4 demonstrates a double logarithmic plot of the experimental data of three-point bending strength and biaxial strength for Weibull analysis. The data points fell approximately along a straight line, revealing that the two-parameter Weibull distribution was a reasonable assumption for the strength distribution of the five samples. When subjected to three-point bending stress, the Weibull modulus decreased from the 17.9 down to 10.2 with increasing CaSi amount in the composites (Table 1). In the case of biaxial stress mode, the Weibull modulus values were similar but showed an appreciable reduction for the higher CaSi composite implants.

5.3. In vitro degradation

5.3.1. Phase composition and microstructure

The potential variations in the properties of the materials during long-term soaking in a physiological solution were addressed. After soaking in the SBF solution, there were no obvious changes for all samples with the increasing soaking time in the resulting XRD patterns (Fig. 5). Similarly, the FTIR spectra of all samples did not change significantly throughout soaking periods up to 12 months (Fig. 6).

The failure to see significant changes in the XRD patterns did not necessarily imply that nothing had happened at the very surface during soaking in an SBF solution. The difficulty for XRD to detect small changes on immersed surfaces was largely resolved by utilizing the SEM technique. After soaking in SBF for 12 months, the surface morphology of all samples was found to alter with the presence of numerous etching-induced micropores, in particular, for higher CaSi content specimens (Fig. 7).

5.3.2. Weight loss

The effect of the soaking time on the weight loss of the samples is presented in Fig. 8. There were almost no weight changes during the soaking time, independent on the types of osteo-implants. At the end of the soaking duration (12 months), the weight loss of approximately 0.1%, 0.3%, 0.2%, 0.1%, and 0.4% were measured for ZCS0, ZCS5, ZCS10, ZCS15, and ZCS20, respectively.

5.3.3. Biaxial flexural strength

The relationship between the CaSi content and the biaxial flexural strength of the implants after soaking in an SBF solution is shown in Fig. 9. The results revealed that soaking time did not significantly ($p < 0.05$) affect the biaxial strength of all groups.

5.4. In vitro osteogenic activity

5.4.1. Cell attachment and proliferation

The quantification of adherent MG63 cells on different surfaces was performed using the MTT assay. Fig. 10 presents that the absorbance steadily increases in all of the samples on hour 6 through day 7, which indicates the increasing number of viable cells. Of note, the cell attachment and proliferation gradually increased with increasing amount of CaSi added to ZrO_2. As expected, the cell attachment and growth to the composite ceramics were faster than those observed in the ZrO_2 control. More cells initially attached to the 20 wt% CaSi-containing composite (ZCS20) than the ZCS0 control during initial 1 day culture, indicating a statistically significant difference ($p < 0.05$). On day 7, ZCS20 revealed a significant ($p < 0.05$) increase of approximately 35% in the absorbance value referenced to the control.

5.4.2. Cell differentiation

The ALP activity was monitored for up to 14 days to investigate the influence of composition formulation on cell differentiation. The cells seeding on the higher CaSi content implants produced greater ALP levels than the cells on the lower CaSi content samples at all culture times (Fig. 11). On day 14, a significant increase ($p < 0.05$) in the ALP level was measured for ZCS15 and ZCS20 compared to ZCS0.

5.4.3. Mineralization

Quantification of calcium mineral deposits by the Alizarin Red S assay showed that with increasing culture time, mineral deposition increased for the cells cultured on all samples (Fig. 12). Greater mineral deposition was found for samples with higher CaSi content. The calcium content in the 15 and 20 wt% CaSi-containing osteo-implants was significantly ($p < 0.05$) higher than those obtained for the ZCS0 seeded with cells after 7 and 14 days of culture.

6. Discussion

Much effort has been dedicated to designing osteo-implants to match the mechanical and osteogenic properties of the repaired bone tissue. In this study, the incorporation of CaSi into zirconia was developed and corresponding mechanical properties, long-term *in vitro* degradation, and osteogenic activity aiming at bone implant applications was

determined. All samples indicated t-ZrO_2 as the dominant phase associated with relatively small m-ZrO_2 amount. The CaSi components did not affect the tetragonal-monoclinic phase transformation of ZrO_2, although a diffusion reaction between Ca/Si and ZrO_2 to form the small amounts of secondary phases such as calcium silicate, calcium zirconium silicate, and calcium zirconate was detected. Stabilization of t-ZrO_2 has been observed at high temperatures when low percentages of calcia (CaO), magnesia (MgO), and yttria (Y_2O_3) are incorporated for the preparation of binary oxides [34]. Shuai *et al.* found that the addition of $CaSiO_3$ to nano-ZrO_2 scaffolds promoted the phase transformation of monoclinic phase (m-ZrO_2) into tetragonal phase (t-ZrO_2) [35]. On the other hand, the formation of micropores on the higher CaSi-containing implant surface was possibly due to grinding effect of fragile CaSi powder [36].

Given that mechanical properties of commonly used ZrO_2 materials are far greater than those of the cortical bone, uneven stress concentrations and easy bone fracture may occur due to difference in strength, when bonding to a host bone [20]. Ideally, the flexural strength and modulus of the developed implant materials should be comparable to those of the replaced cortical bone (bending strength: 50–150 MPa, Young's modulus: 7–30 GPa) [37]. In this study, the biaxial flexural strength and three-point bending strength of the composite implants with a CaSi content of up to 10 wt% hardly changed when compared to those of the ZrO_2 control, but it decreased markedly at 15 wt% CaSi. This decrease can be due to the inherent low mechanical strength and Young's modulus of the CaSi component, acting more or less like structure flaws [17], which was evidenced by SEM. It is reasonable to suggest that microstructural and mechanical characteristics strongly depended on preparation conditions such as the additive content and sintering temperature. The surface characterization of CaSi was affected by the sintering temperature [29]. It is worthwhile to note that 15 and 20 wt% CaSi-containing composite osteo-implants had average three-point bending strength values of 162 and 132 MPa, respectively, which was within the reported bending strength for cortical bone [37]. Additionally, the ZrO_2 control had a lower bending or biaxial strength than those reported in the previous studies [38–40]. This can arise from the differences in the used raw material, sintering temperature, and applied pressure [38–40]. It is well known that strength could be improved by increasing the sintering temperature and applied pressure, which may favor coalescence of the powders. Regarding Weibull modulus (m), larger values implied more reliably reproducible materials in a narrower distribution of values. The lower value represents more flaws and defects in the tested material and thus less reliability. Most ceramics are reported to have m values in the range of 5–15 [27]. Weibull modulus identified in the control is consistent with an earlier study that reported Weibull modulus values ranging from 9.8 to 12.9 for Y-TZP using biaxial test [39].

The improvement of the mechanical features of load-bearing materials is fundamental to reach an equilibrated biomechanical loads distribution at the bone-implant interface and reducing mismatch to favor the osteointegration process [41]. When the implant material has a higher Young's modulus than bone, they can cause stress shielding and lead to bone resorption [42–44]. Elastic modulus of commercial ZrO_2 (200 GPa) products are around ten times greater than that of cortical bone (about 20 GPa). This disparity leads to complications in biomechanical compatibility between ZrO_2 implant and bone tissue. In a word, the higher elastic modulus of ZrO_2 than that of cortical bone can cause stress concentrations within the surrounding bone tissue, resulting in bone fractures and reduced device lifetime. Hence, further research is required to develop a high efficacy zirconia-based material candidate with elastic modulus comparable to that of the cortical bone. In fact, introducing micro-pores into the structure [17,20] and development of composite may reduce the Young's modulus of the ZrO_2 implant. In the case of the composite implants, the incorporation of CaSi indeed reduced the modulus of the ZrO_2. For example, the addition of 15 wt% CaSi lowered the modulus of the ZrO_2 control by about 20%. Intrinsically, the CaSi component was not stiffer than the surrounding ZrO_2 ceramic matrix, it was reasonable to speculate that the modulus of the composite implants decreased with the increasing CaSi content.

According to the literature [45], the ZrO_2 material should possess long-term clinical survival and be in service within the oral environment for many years. Since ZrO_2 is sensitive to slow crack growth and aging; thus, it is important to perform degradation test to insure superior stability at long durations in contact with body fluid. Biodegradation of biomaterials can be characterized by changes in the physicochemical properties and mechanical strength of the materials after implantation or after soaking in a physiological solution [46]. One concern was that the incorporation of CaSi might result in degradation of the properties of the novel implant systems. The present results indicated that the long-term soaking in the pH 7.4 SBF solution did not remarkably influence the phase composition from the resulting XRD patterns and FTIR spectra, and biaxial strength. The continuous impact of water molecules from SBF into the lattice sites of t-ZrO_2 did not give rise to in the t-m phase transformation for all groups.

When soaked in the dynamic SBF solution, the ZrO_2 control has a considerably small ionic release from the result of weight loss, consistent with *in vivo* results [47], although numerous etching-induced micropores on the implant surfaces were found. This can be explained by the fact that water/ions easily infiltrated the inner portion of the material through structural imperfections. Concerning the composite, the greatest CaSi content in the ZCS20 sample had the highest weight loss because the release of soluble fractions (CaSi), but it revealed a relatively small degree of weight loss of less than 1%

even after a 12-month soaking time. The extremely low-degradation ability of the ZrO_2-based implant systems was necessary for a long-term clinical application. As expected, the CaSi components can be preferably dissolved when compared to the ZrO_2 matrix. Ionic dissolution products of CaSi-based ceramics could lead to mineral deposition at the material-bone interface [48].

The implant materials should support cell and tissue growth, enhancing osteogenesis. Zirconia is used for dental applications because of its low toxicity and beneficial mechanical properties, but it has no biological activities and is covered by a non-adherent fibrous layer at the interface after implantation [14,19,20]. Intriguing research is to focus on zirconia-based materials alternative to Y-TZP, especially for long-term implantation applications for which the osteogenesis is of importance. Matsumoto *et al.* fabricated a composite material having compressive strength similar to cortical bone with high cell and tissue affinities by compounding ZrO_2 and hydroxyapatite [20]. Cell functions associated with an implant are closely related to the surface chemistry of the materials used [3,22,49]. To elucidate the effects of the CaSi additives on osteogenic activity, cell attachment, proliferation, differentiation, and mineralization of MG63s cultured on the various osteo-implants were evaluated.

First of all, the initial responses of MG63 cells on the various material surfaces were evaluated, which early cell-material interactions affected subsequent differentiation and mineralization. Cell attachment and proliferation on higher CaSi implants were significantly higher than those on the control without CaSi. The results of the present study clearly demonstrated that CaSi was an effective promoter of biological functions of cells in supporting the attachment and proliferation of MG63s. Cell differentiation studies, like cell proliferation assay results, also showed a significant impact of CaSi, with an emphasis on the importance of material compositions [3]. Indeed, ALP activity increased with increasing CaSi content in the composite osteo-implants. ALP enzyme activity is also associated with bone formation, and it is produced in high levels during the bone formation phase [24]. An increase in the specific activity of ALP in bone cells reflects a shift to a more differentiated state.

To more fully assess the role of CaSi in cell function, mineralization ability was assayed. Alizarin Red S staining is a common histochemical technique used for detecting calcium deposits in mineralized tissues and cultures [12,50]. The ability of cells to produce a mineralized matrix and nodules in materials is important for bone regeneration. Among the five samples, mineralized nodule formation was most noticeable on the higher CaSi implant surfaces, speculating that this composite implant will produce more mineralized tissue formation upon implantation. Recent studies also show that calcium silicate could stimulate the mineralization [22]. Overall, the increased proliferation,

differentiation, and mineralization of MG63 cells consistently addressed that the CaSi component in the ZrO_2-based implants was responsible for the enhanced cell growth, which enhanced its potential clinical applications.

7. Conclusions

For the first time, a series of ZrO_2 composite implants containing calcium silicate have been evaluated to enhance the osteogenesis of the ZrO_2 osteo-implant. In light of the results obtained in this study, a bioactive calcium silicate not only reduced the modulus of tough ZrO_2 implant, but also it enhanced biologic properties of the implants. Taking the mechanical properties and osteogenic activity into account, 15 wt% calcium silicate-containing ZrO_2 implant was the best choice for cortical bone repair. The current work opens up possibilities of producing high bioactive calcium silicate-ZrO_2 composite implant with a mechanical compatibility that can meet the reconstruction requirement of cortical bone.

7. Evaluation

The three-year project focuses on evaluation of mechanical properties, in vitro degradation and osteogenesis of ZrO_2–based composite implants. The results have been accepted by Applied Materials Today. Nevertheless, the further investigation on the development of bioactive ZrO_2 bone implants with antibacterial activity will be needed in the future.

8. 參考文獻

[1] M. Geetha, A.K. Singh, R. Asokamani, A.K. Gogia, Ti based biomaterials, the ultimate choice for orthopaedic implants – a review, Prog. Mater. Sci. 54 (2009) 397–425.

[2] C.C. Ho, S.J. Ding, Novel SiO2/PDA hybrid coatings to promote osteoblast-like cell expression on titanium implants, J. Mater. Chem. B 3 (2015) 2698–2707.

[3] C. Hegedűs, C.C. Ho, A. Csík, S. Biri, S.J. Ding, Enhanced physicochemical and biological properties of ion-implanted titanium using electron cyclotron resonance ion sources, Materials 9 (2016) 25.

[4] B. Stadlinger, M. Hennig, U. Eckelt, E. Kuhlisch, R. Mai, Comparison of zirconia and titanium implants after a short healing period. A pilot study in minipigs, Int. J. Oral Maxillofac. Surg. 39 (2010) 585–592.

[5] C.J. Chen, C.C. Chen, S.J. Ding, Effectiveness of hypochlorous acid to reduce the biofilms on titanium alloy surfaces in vitro, Int. J. Mol. Sci. 17 (2016) 1161.

[6] C. Piconi, G. Maccauro, Zirconia as a ceramic biomaterial, Biomaterials 20 (1999) 1–25.

[7] J.R. Kelly, Dental ceramics: current thinking and trends, Dent. Clin. N. Am. 48 (2004) 513–530.

[8] D.D. Bosshardt, V. Chappuis, D. Buser, Osseointegration of titanium, titanium alloy

and zirconia dental implants: current knowledge and open questions, Periodontology 2000 73 (2017) 22–40.
[9] R.C. Garvie, R.H. Hannink, R.T. Pascoe, Ceramic steel? Nature 258 (1975) 703–704.
[10] R.H.J. Hannink, P.M. Kelly, B.C. Muddle, Transformation toughening in zirconia containing ceramics, J. Am. Ceram. Soc. 83 (2004) 461–487.
[11] J. Chevalier, What future for zirconia as a biomaterial, Biomaterials 27 (2006) 535–543.
[12] C.C. Wu, C.K. Wei, C.C. Ho, S.J. Ding, Enhanced hydrophilicity and biocompatibility of dental zirconia ceramics by oxygen plasma treatment, Materials 8 (2015) 684−699.
[13] R.J. Kohal, D. Weng, M. Bachle, J.R. Strub, Loaded custom-made zirconia and titanium implants show similar osseointegration: an animal experiment, J. Periodontol. 75 (2004) 1262–1268.
[14] L.L. Hench, Bioceramics: from concept to clinic, J. Am. Ceram. Soc. 74 (1991) 1487–1510.
[15] H. Sakai, T. Asaoka, Development of biocompatible Y-Stabilized ZrO2 fabricated by spark plasma sintering, Adv. Sci. Technol. 86 (2013) 17−21.
[16] A. Pelaez-Vargas, D. Gallego-Perez, M. Magallanes-Perdomo, M.H. Fernandes, D.J. Hansford, A.H. De Aza, P. Pena, F.J. Monteiro, Isotropic micropatterned silica coatings on zirconia induce guided cell growth for dental implants, Dent. Mater. 27 (2011) 581–589.
[17] Z. Shen, E. Adolfsson, M. Nygren, L. Gao, H. Kawaoka, K. Niihara, Dense hydroxyapatite-zirconia ceramic composites with high strength for biological applications, Adv. Mater. 13 (2001) 214–216.
[18] M. Inuzuka, S. Nakamura, S. Kishi, K. Yoshida, K. Hashimoto, Y. Toda, K. Yamashita, Hydroxyapatite-doped zirconia for preparation of biomedical composites ceramics, Solid State Ionics 172 (2004) 509–513.
[19] J. Marchi, V. Ussui, C.S. Delfino, A.H.A. Bressiani, M.M. Marques, Analysis in vitro of the cytotoxicity of potential implant materials. I: zirconia–titania sintered ceramics, J. Biomed. Mater. Res. B 94 (2010) 305–311.
[20] T. J. Matsumoto, S.-H. An, T. Ishimoto, T. Nakano, T. Matsumoto, S. Imazato, Zirconia–hydroxyapatite composite material with micro porous structure, Dent. Mater. 27 (2011) e205–e212.
[21] J.R. Jones, Review of bioactive glass: from Hench to hybrids, Acta Biomater. 9 (2013) 4457–4486.
[22] S.C. Huang, B.C. Wu, S.J. Ding, Stem cell differentiation-induced calcium silicate cement with bacteriostatic activity, J. Mater. Chem. B 3 (2015) 570−580.
[23] N. Zhang, J.A. Molenda, J.H. Fournelle, W.L. Murphy, N. Sahai, Effects of pseudowollastonite (CaSiO3) bioceramic on in vitro activity of human mesenchymal stem cells, Biomaterials 31 (2010) 7653−7665.
[24] S.J. Ding, M.Y. Shie, C.K. Wei, In vitro physicochemical properties, osteogenic activity, and immunocompatibility of calcium silicate-gelatin bone grafts for load-bearing applications, ACS Appl. Mater. Interfaces 3 (2011) 4142−3153.
[25] S. Xu, K. Lin, Z. Wang, J. Chang, L. Wang, J. Lu, C. Ning, Reconstruction of calvarial defect of rabbits using porous calcium silicate bioactive ceramics, Biomaterials 29 (2008) 2588−2596.

[26] ISO 6872: 2008 Dentistry – Ceramic materials.
[27] C.K. Wei, S.J. Ding, Acid-resistant calcium silicate-based composite implants with high-strength as load-bearing bone graft substitutes and fracture fixation devices, J. Mech. Behav. Biomed. Mater. 62 (2016) 366−383.
[28] R. Ianoş, P. Barvinschi, Solution combustion synthesis of calcium zirconate, CaZrO3, powders, J. Solid State Chem. 183 (2010) 491–496.
[29] C.C. Chen, C.C. Ho, S.Y. Lin, S.J. Ding, Green synthesis of calcium silicate bioceramic powders, Ceram. Int. 41 (2015) 5445–5453.
[30] T.C. Schumacher, E. Volkmann, R. Yilmaz, A. Wolf, L. Treccani, K. Rezwan, Mechanical evaluation of calcium-zirconium-silicate (baghdadite) obtained by a direct solid-state synthesis route, J. Mech. Behav. Biomed. Mater. 34 (2014) 294–301.
[31] P.R. Lee, C.C. Ho, C.S. Hwang, S.J. Ding, Improved physicochemical properties and biocompatibility of stainless steel implants by PVA/ZrO_2-based composite coatings, Surf. Coat. Technol. 258 (2014) 374–380.
[32] J. Marchi, E.M. Amorim, D.R.R. Lazar, V. Ussui, A.H.A. Bressiani, P.F. Cesar, Physico-chemical characterization of zirconia–titania composites coated with an apatite layer for dental implants, Dent. Mater. 29 (2013) 954–962.
[33] L. Armelao, S. Gross, K. Müller, G. Pace, E. Tondello, O. Tsetsgee, A. Zattin, Structural evolution upon thermal heating of nanostructured inorganic-organic hybrid materials to binary oxides MO_2SiO_2 (M=Hf, Zr) as evaluated by solid-state NMR and FTIR spectroscopy, Chem. Mater. 18 (2006) 6019–6030.
[34] F. del Monte, W. Larsen, J.D. Mackenzie, Chemical interactions promoting the ZrO2 tetragonal stabilization in ZrO_2–SiO_2 binary oxides, J. Am. Ceram. Soc. 83 (2000) 1506–1512.
[35] C. Shuai, P. Feng, B. Yang, Y. Cao, A. Min, S. Peng. Effect of nano-zirconia on the mechanical and biological properties of calcium silicate scaffolds, Int. J. Appl. Ceram. Technol. 12 (2015) 1148–1156.
[36] C.C. Chen, M.H. Lai, W.C. Wang, S.J. Ding, Properties of anti-washout-type calcium silicate bone cements containing gelatin, J. Mater. Sci. Mater. Med. 21 (2010) 1057−1068.
[37] T. Kokubo, H.-M. Kim, M. Kawashita, Novel bioactive materials with different mechanical properties, Biomaterials 24 (2003) 2161–2175.
[38] M. Guazzato, M. Albakry, S.P. Ringer, M.V. Swain, Strength, fracture toughness and microstructure of a selection of all-ceramic materials. Part II. Zirconia-based dental ceramics, Dent. Mater. 20 (2004) 449–456.
[39] P. Pittayachawan, A. McDonald, A. Petrie, J.C. Knowles, The biaxial flexural strength and fatigue property of LavaTM Y-TZP dental ceramic, Dent. Mater. 23 (2007) 1018–1029.
[40] H. Sato, K. Yamada, G. Pezzotti, M. Nawa, S. Ban, Mechanical properties of dental zirconia ceramics changed with sandblasting and heat treatment, Dent. Mater. J. 27 (2008) 408–414.
[41] S. Sprio, A. Tampieri, G. Celotti, E. Landi, Development of hydroxyapatite/calcium silicate composites addressed to the design of load-bearing bone scaffolds, J. Mech. Behav. Biomed. Mater. 2 (2009) 147–155.
[42] W.R. Moore, S.E. Graves, G.I. Bain, Synthetic bone graft substitutes, ANZ J. Surg.

71 (2001) 354−361.
[43] N.M. Alves, I.B. Leonor, H.S. Azevedo, R.L. Reis, J.F. Mano, Designing biomaterials based on biomineralization of bone, J. Mater. Chem. 20 (2010) 2911–2921.
[44] A.R. Dujovne, J.D. Bobyn, J.J. Krygier, J.E. Miller, C.E. Brooks, Mechanical compatibility of noncemented hip prostheses with the human femur, J. Arthroplast. 8 (1993) 7–22.
[45] E. Siarampi, E. Kontonasaki, K.S. Andrikopoulos, N. Kantiranis, G.A. Voyiatzis, T. Zorba, K.M. Paraskevopoulos, P. Koidis, Effect of in vitro aging on the flexural strength and probability to fracture of Y-TZP zirconia ceramics for all-ceramic restorations, Dent. Mater. 30 (2014) e306–e316.
[46] A.A. Barros, C. Oliveira, E. Lima, A.R. C. Duarte, R.L. Reis, Gelatin-based biodegradable ureteral stents with enhanced mechanical properties, Appl. Mater. Today 5 (2016) 9–18.
[47] Y. Ichikawa, Y. Akagawa, H. Nikai, H. Tsuru, Tissue compatibility and stability of a new zirconia ceramic in vivo, J. Prosthet. Dent. 68 (1992) 322–326.
[48] M.G. Gandolfi, P. Taddei, S. Siboni, E. Modena, E.E. de Stefano, C. Prati, Biomimetic remineralization of human dentin using promising innovative calcium-silicate hybrid “smart” materials, Dent. Mater. 27 (2011) 1055–1069.
[49] G. Pezzotti, R.M. Bock, T. Adachi, A. Rondinella, F. Boschetto, W. Zhu, E. Marin, B. McEntire, B. Sonny Bal, O. Mazdafa, Silicon nitride surface chemistry: a potent regulator of mesenchymal progenitorcell activity in bone formation, Appl. Mater. Today 9 (2017) 82–95.
[50] P. Bhattacharjee, D. Naskar, T.K. Maiti, D. Bhattacharya, S.C. Kundu, Investigating the potential of combined growth factors delivery, from non-mulberry silk fibroin grafted poly(ε-caprolactone)/hydroxyapatite nanofibrous scaffold, in bone tissue engineering, Appl. Mater. Today 5 (2016) 52–67.

Table 1

Mechanical property of the ZrO_2-based composite osteo-implants as a function of the CaSi content.

Sample code	Three-point bending			Biaxial strength	
	Strength (MPa)	Young's modulus (GPa)	Weibull modulus	Strength (MPa)	Weibull modulus
ZCS0	186±11[a]	24.5±2.4[a]	17.9	335±29[a]	12.4
ZCS5	194±12[a]	22.4±3.2[a,b,c]	17.3	354±36[a]	10.5
ZCS10	192±13[a]	23.1±5.2[a,b]	15.0	324±23[a]	14.7
ZCS15	162±16[b]	20.1±4.8[b,c]	10.6	223±24[b]	9.7
ZCS20	132±14[c]	19.0±4.3[c]	10.2	164±18[c]	9.8

Mean values followed by different superscript letters were significantly different ($p < 0.05$) according to Scheffé *post hoc* multiple comparisons.

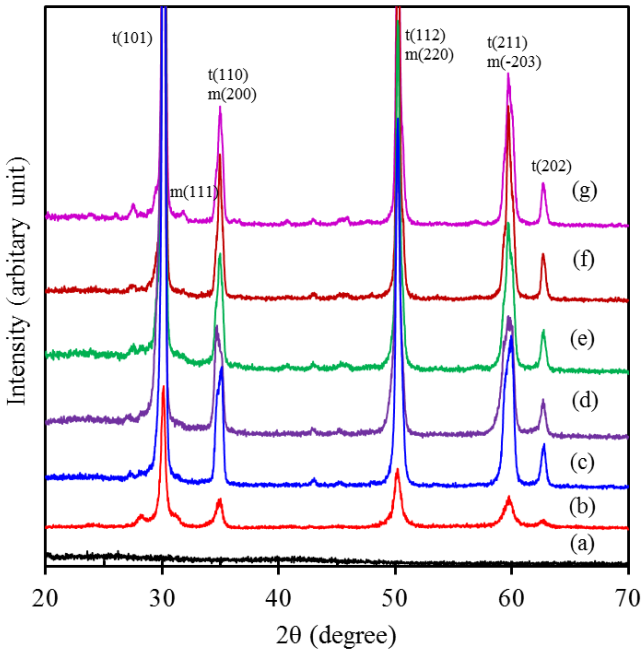

Fig. 1. XRD patterns of (a) calcium silicate (CaSi) gel powder, (b) as-received ZrO_2 powder, and sintered ZrO_2 osteo-implants with (c) 0, (d) 5, (e) 10, (f) 15, and (g) 20 wt% CaSi.

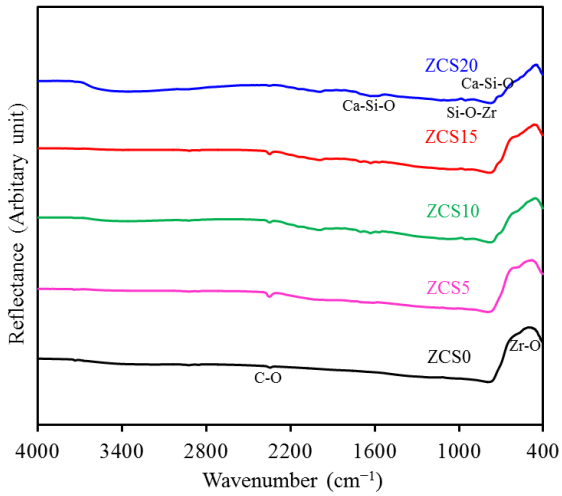

Fig. 2. FTIR spectra of various sintered ZrO_2 osteo-implants containing different CaSi content.

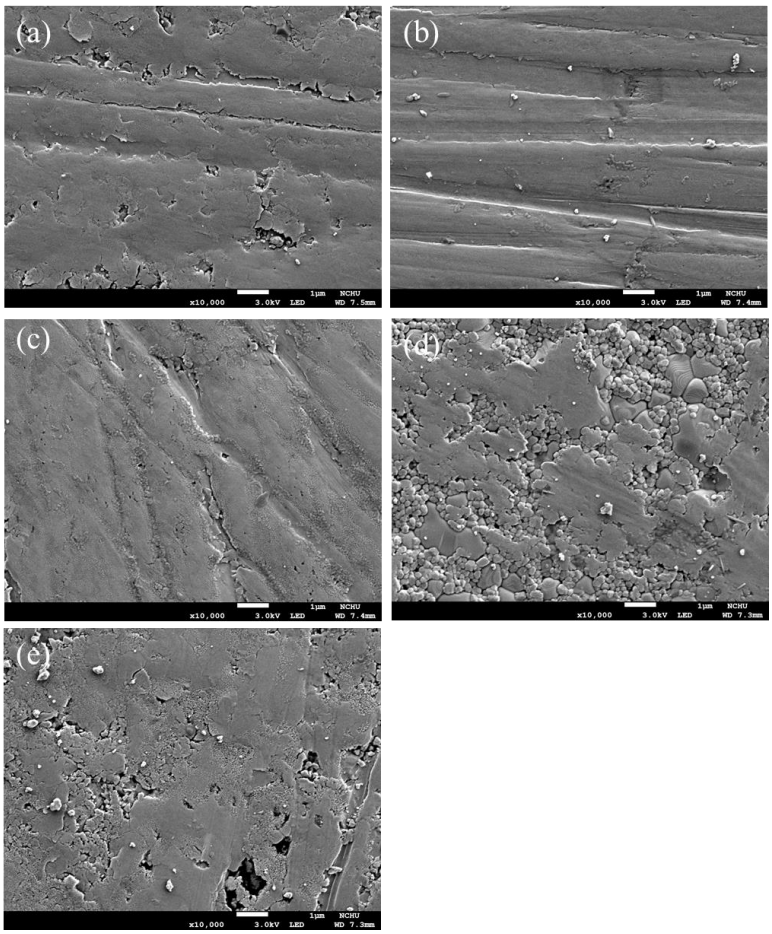

Fig. 3. Surface SEM images of sintered ZrO_2 osteo-implants containing (a) 0, (b) 5, (c) 10, (d) 15, and (e) 20 wt% CaSi.

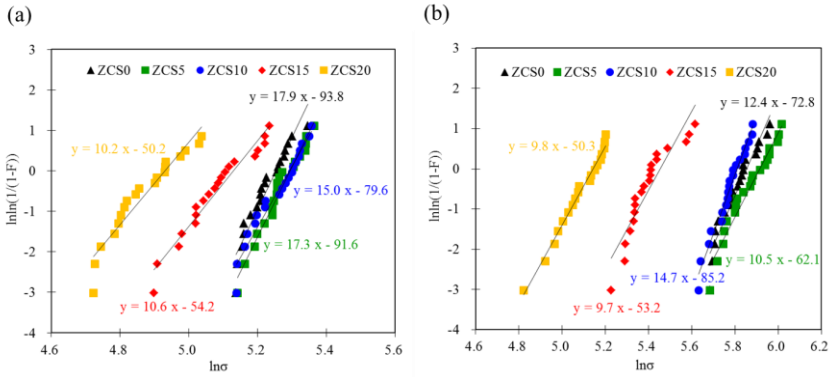

Fig. 4. Weibull strength distribution plots of various sintered ZrO_2 osteo-implants containing different CaSi content subjected to (a) three-point bending and (b) biaxial tests. F is the failure probability and σ is the strength. The solid line represents the regression line.

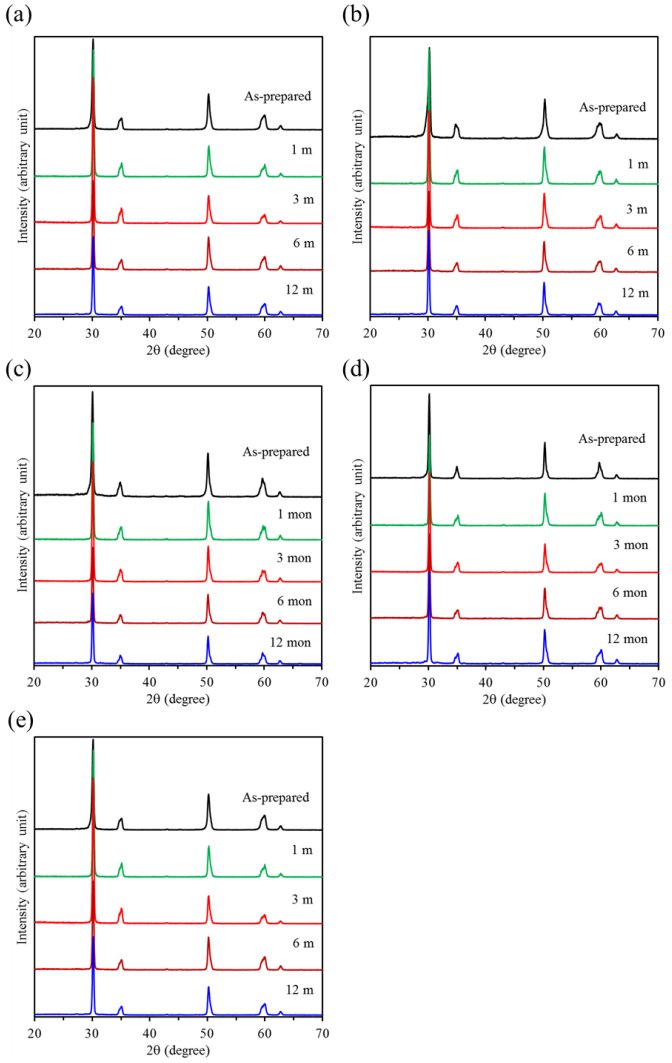

Fig. 5. XRD patterns of various ZrO_2 osteo-implants containing (a) 0, (b) 5, (c) 10, (d) 15, and (e) 20 wt% CaSi before and after soaking in an SBF solution for predetermined time durations.

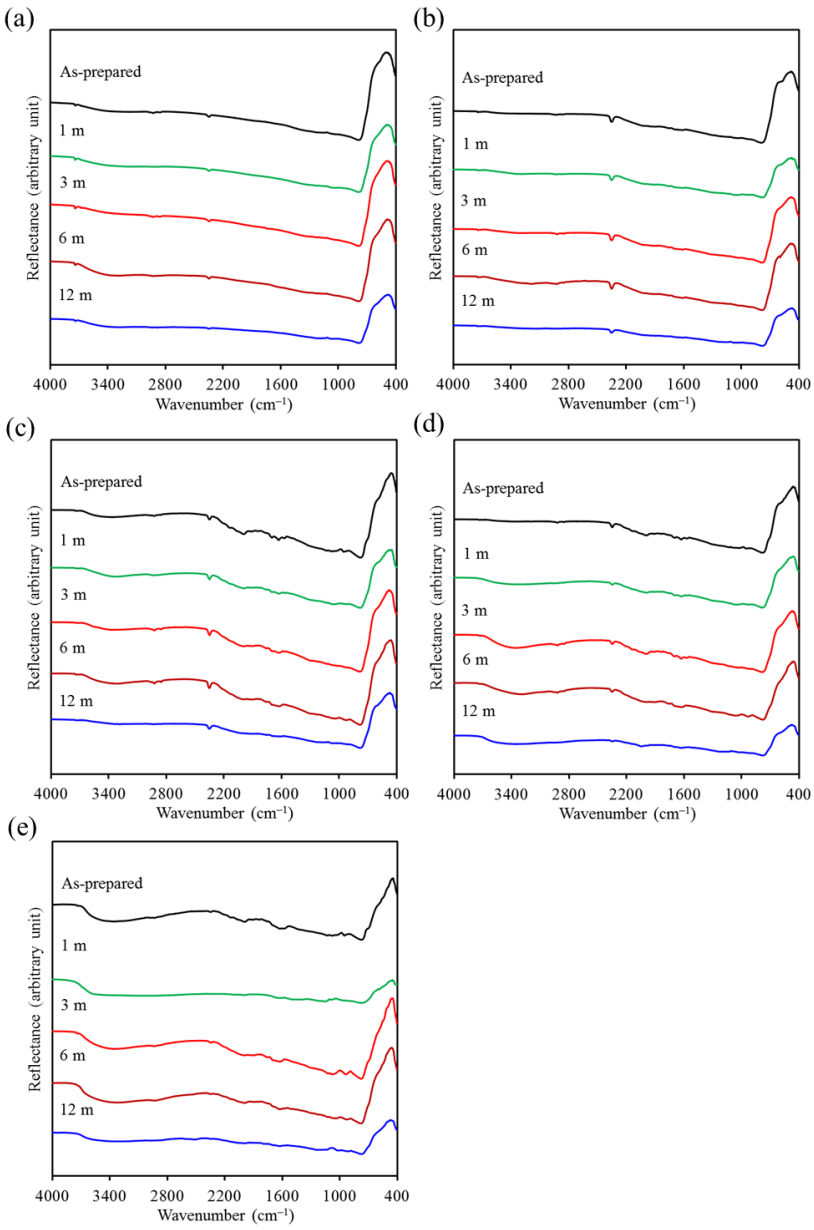

Fig. 6. FTIR spectra of various ZrO_2 osteo-implants containing (a) 0, (b) 5, (c) 10, (d) 15, and (e) 20 wt% CaSi before and after soaking in an SBF solution for predetermined time durations.

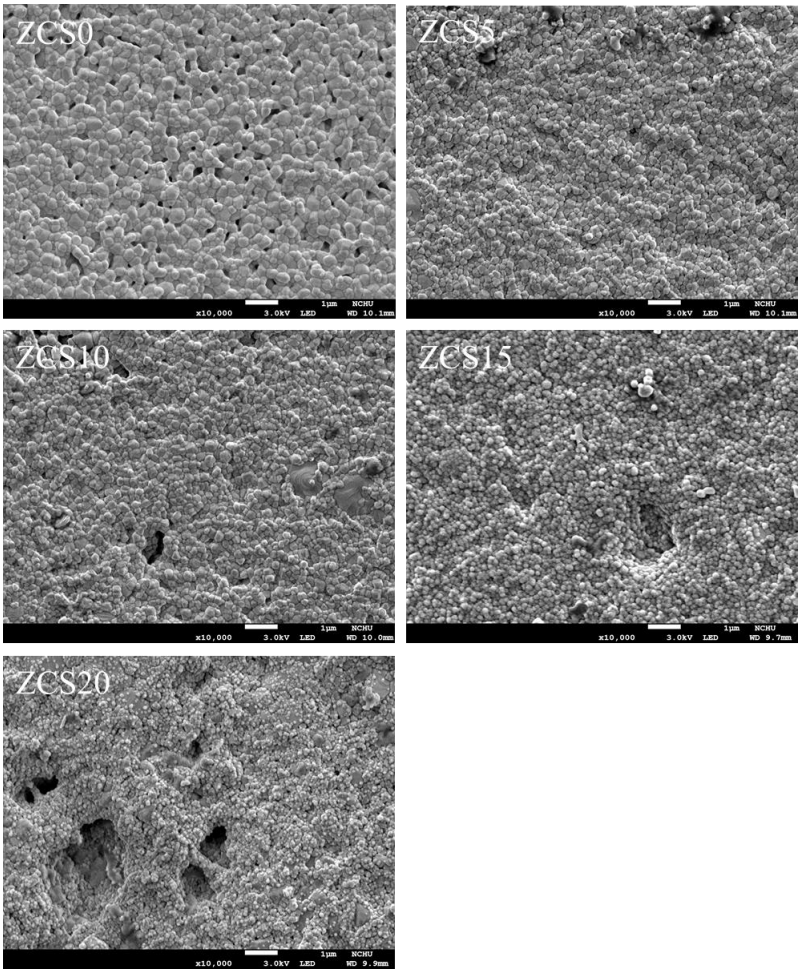

Fig. 7. Surface SEM images of various ZrO_2 osteo-implants containing different CaSi content after soaking in an SBF solution for 12 months.

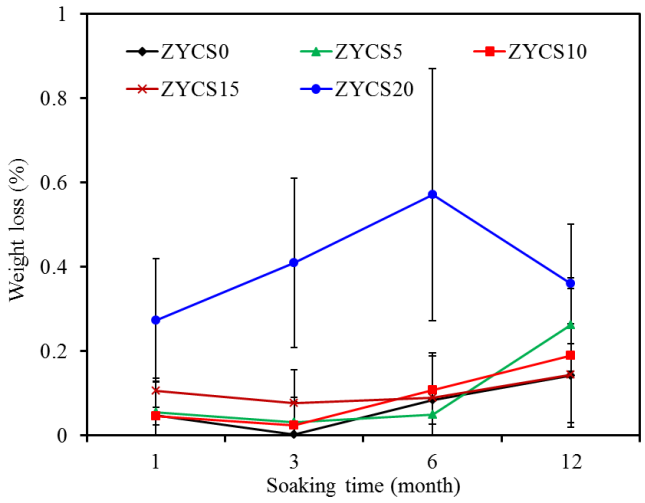

Fig. 8. Weight loss of various ZrO_2 osteo-implants containing different CaSi content after soaking in an SBF solution for predetermined time durations.

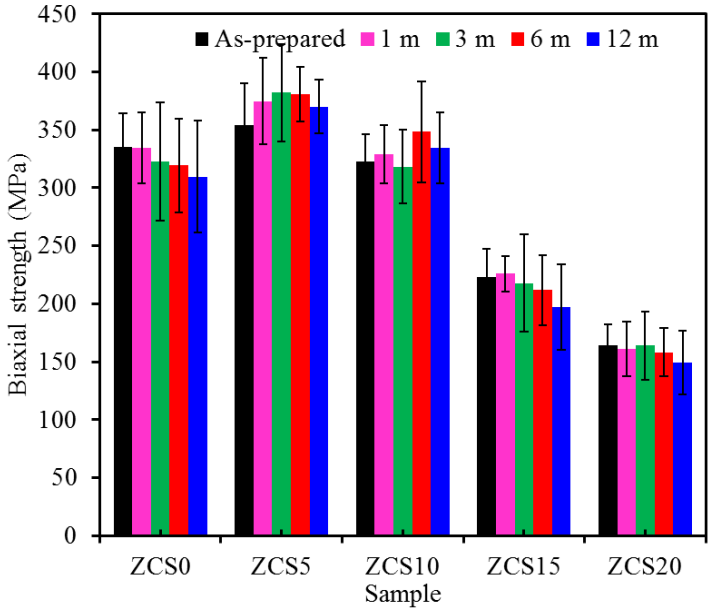

Fig. 9. Biaxial flexural strength of various ZrO_2 osteo-implants containing different CaSi content before and after soaking in an SBF solution for predetermined time durations.

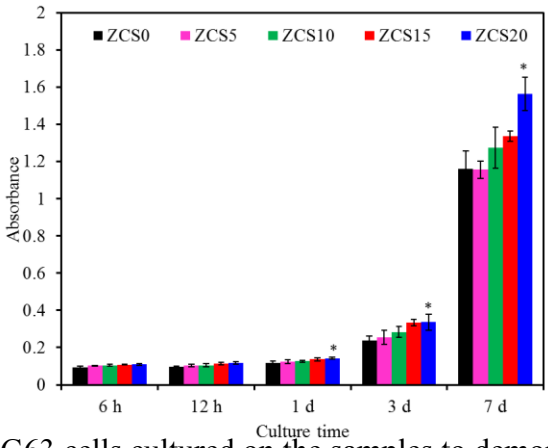

Fig. 10. MTT assay of MG63 cells cultured on the samples to demonstrate cell attachment and proliferation at various culture time points. *Statistically significant difference ($p < 0.05$) from the ZCS0 control.

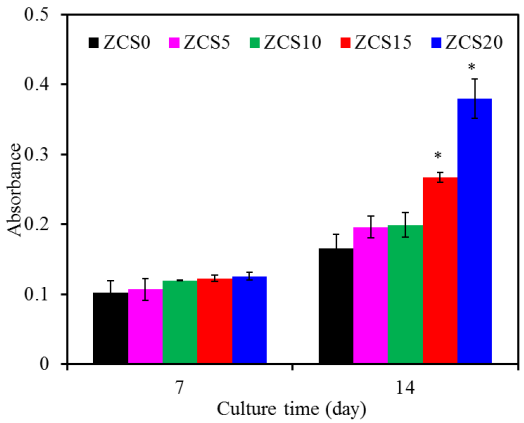

Fig. 11. ALP assay on MG63 cells presented as absorbance for cell differentiation on various samples after 7 and 14 days of culture. *Statistically significant difference ($p < 0.05$) from the ZCS0 control.

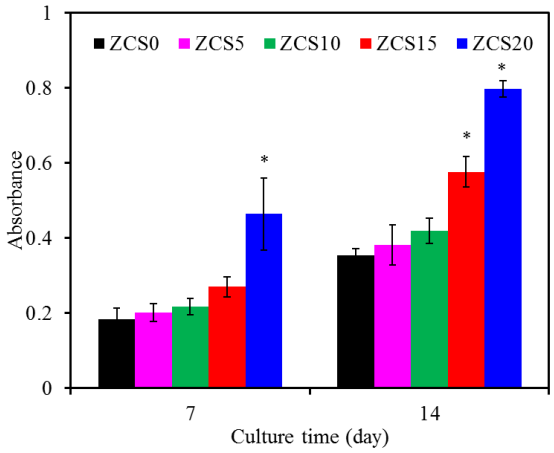

Fig. 12. Quantification of calcium mineral deposits by Alizarin Red S assay of MG63 cells cultured on various samples after culture for 7 and 14 days. *Statistically significant difference ($p < 0.05$) from the ZCS0 control.

出席國際學術會議心得報告

計畫編號	MOST 104-2221-E-040-004-MY3
計畫名稱	荷重型高骨形成性生物陶瓷複合材料研發
出國人員姓名 服務機關及職稱	丁信智 中山醫學大學　口腔科學研究所　教授
會議時間地點	106/9/4-8　希臘雅典
會議名稱	第 28 屆歐洲生醫材料研討會
發表論文題目	Novel ZrO_2-based implant systems with high osteogenic activity

一、參加會議經過

2017 年第 28 屆歐洲生醫材料研討會在希臘雅典的國際會議廳舉行。7 場 plenary lectures 包含 N.A. Peppas, A.G. Mikos, D. Letourneur, J.A. Jansen, D.W. Hutmacher, L. Ambrosio 等國際知名人物。會議期間有及 G. Winter 及 40 歲以下的年輕學者獎之得獎者的專題演講。整個會議研討涵蓋與生醫材料相關的各種不同議題，如組織工程、表面修飾、仿生材料、鈣磷陶瓷、降解性高分子、生物相容性研究、蛋白質吸附、奈米複合材、基因藥物治療研究等。並有生醫材料製造、儀器設備商、及書商同時參展，會場討論氣氛十分熱絡。

二、與會心得

此研討會主要是由歐洲生醫材料學會主導，除歐洲地區生醫材料學者參加外，美加及亞洲地區多位學者亦參與。較少見台灣學者。生醫材料研究為一跨領域且理論、應用並重的學門，從與會中所發表的論文可知仍有相當大的研究空間，但有待臨床醫師與生醫材料研究者雙向交流與合作，才能更加突破目前所面臨之瓶頸。從國外學者的研究趨勢及發表主題，顯示台灣生醫材料界研究方向與世界並進、並未偏離。本次參與研討會也與國外學者進行多次意見交流。

Novel ZrO_2-based implant systems with high osteogenic activity

Shinn-Jyh Ding, Ying-Hung Chu, De-Yu Wang

Institute of Oral Science, Chung Shan Medical University, Taiwan
sjding@csmu.edu.tw

INTRODUCTION

Zirconia has been currently used in the femoral head of hip prostheses and dental restoration because of its excellent mechanical properties, good abrasion resistance and chemical stability. However, this material has no direct bone bonding properties or osteogenesis. To pursue the high bone bonding ability is still a concerned theme, although commercial ZrO_2 systems are available today. Calcium silicate-based bone graft substitutes have been developed for hard tissue applications. Newly formed bone tissue can grow on the surface of the calcium silicate-based materials, along with the deposition of a bone-like apatite layer at the tissue/material interface[1]. To improve the osteogenesis of the dental zirconia ceramics, the incorporation of the calcium silicate into zirconia was developed. The objective of the study was to assess the effect of calcium silicate on the physicochemical properties and in vitro osteogenic activity of the ZrO_2-based ceramics.

EXPERIMENTAL METHODS

The details of the procedure for the preparation of the sol-gel-derived calcium silicate powder as a starting material have been described elsewhere[2]. This dried calcium silicate powders was added to the ZrO2 powder at 5, 10, 15, and 20 wt% using a mixer and then ball-milled for 5 h in ethyl alcohol and dried in an oven over night. After this, the green bodies were sintered using a high-temperature furnace, then furnace-cooled to room temperature.

Phase analysis was performed using an X-ray diffractometer (XRD). A digital microhardness tester with a four-sided diamond pyramid was used to evaluate the Vickers hardness (Hv) of the various specimens. MG63 human osteoblast-like cells were used to evaluate cell behaviour. MG63 cell suspensions at a density of 5×103 cells/mL were seeded over each of the samples. After different culture time points, cell viability was examined using the MTT (3-(4,5-dimethylthiazol-2-yl)-2,5-diphenyltetrazolium bromide). In addition, alkaline phosphatase (ALP) activity and calcium quantification were also evaluated to understand in vitro osteogenic activity. One-way analysis of variance (ANOVA) was used to evaluate significant differences between means in the measured data. In all cases, results were considered statistically significant for a p-value of less than 0.05.

RESULTS AND DISCUSSION

The XRD results indicated that three characteristic peaks located at around 30.2°, 34.6° and 49.9° can be attributed to (101), (110) and (112) tetragonal crystal faces of ZrO2 (t-ZrO2). The calcium silicate-related phases such as calcium silicate, calcium zirconium silicate, silica and calcium oxide were not found, indicating the phase stability of the t-ZrO2 phase by the addition of

calcium silicate. The Hv values of the five samples decreased with increasing calcium silicate content of the composites in the range of 718-457, indicating significant differences ($p < 0.05$). It can be noted that the doped calcium silicate can make the ZrO_2 implant softened.

The bone implant materials should support cell and tissue growth. To elucidate the effects of the addition of calcium silicate on in vitro osteogenic activity, firstly we investigated MG63 cell viability on the composites. As a result, the absorbance steadily increased in all of the specimens on hour 6 through day 7, which indicated the increasing number of viable cells. Of note, the cell viability gradually increased with increasing amount of added calcium silicate. Cell differentiation studies, like cell viability assay, showed a significant impact of calcium silicate, with an emphasis on the importance of material composition. Unsurprisingly, ALP activity increased with increasing calcium silicate content. The results of mineralization ability confirmed that the more calcium silicate, the higher calcium deposits were. There is a statistically significant difference ($p < 0.05$) in cell viability, differentiation and mineralization levels between the implant specimens. The increased cell viability, differentiation, and mineralization ability of MG63 consistently showed that the doped calcium silicate in the ZrO_2 implants was responsible for the cell growth, which was the purpose of this study.

CONCLUSION

A novel ZrO_2–based implant system was developed. In light of the present results, it is concluded that in vitro osteogenic activity of the ZrO2 implants were effectively increased because of calcium silicate.

REFERENCES

1. Xu S. et al., Biomaterials 29:2588−2596, 2008.
2. Ho C.C. et al., Ceram. Int. 42:9183−9189, 2016.

ACKNOWLEDGMENTS

The authors would like to thank the National Science Council of the Republic of China under the Grant No. MOST 104-2221-E-040-004-MY3 for providing financial support to this project.

104年度專題研究計畫成果彙整表

計畫主持人：丁信智	**計畫編號：**104-2221-E-040-004-MY3
計畫名稱：荷重型高骨形成性生物陶瓷複合材料研發	

成果項目					量化	單位	質化 （說明：各成果項目請附佐證資料或細項說明，如期刊名稱、年份、卷期、起訖頁數、證號...等）
國內	學術性論文	期刊論文			0	篇	
		研討會論文			0		
		專書			0	本	
		專書論文			0	章	
		技術報告			0	篇	
		其他			0	篇	
	智慧財產權及成果	專利權	發明專利	申請中	0	件	
				已獲得	0		
			新型/設計專利		0		
		商標權			0		
		營業秘密			0		
		積體電路電路布局權			0		
		著作權			0		
		品種權			0		
		其他			0		
	技術移轉	件數			0	件	
		收入			0	千元	
國外	學術性論文	期刊論文			1	篇	Ding SJ*, YH Chu, Wang DY. Enhanced properties of novel zirconia-based osteo-implant systems. Applied Materials Today 2017;9:622－632.
		研討會論文			3		1. Ding SJ, Chu YH, Wang DY. Novel ZrO2-based implant systems with high osteogenic activity. The 28th Annual Conference of the European Society for Biomaterials (ESB), Athens, Greece, September 4-8, 2017, accepted. 2. Ding SJ, Wang DY. Low degradable calcium silicate/zirconia composite implants with enhanced osteogenesis. 17th Asian BioCeramics Symposium (ABC2017), Okayama, Japan, Nov 30- Dec 1, 2017. 3. Chen PT, Chu YH, Ding SJ. Mechanical properties and

						biocompatibility of calcium silicate-zirconia bone implant systems. 18th Asian BioCeramics Symposium (ABC2018), Bandung, Indonesia, Sept 19-20, 2018.
		專書			0	本
		專書論文			0	章
		技術報告			0	篇
		其他			0	篇
	智慧財產權及成果	專利權	發明專利	申請中	0	件
				已獲得	0	
			新型/設計專利		0	
		商標權			0	
		營業秘密			0	
		積體電路電路布局權			0	
		著作權			0	
		品種權			0	
		其他			0	
	技術移轉	件數			0	件
		收入			0	千元
參與計畫人力	本國籍	大專生			0	人次
		碩士生			0	
		博士生			0	
		博士後研究員			1	Ding SJ*, YH Chu, Wang DY. Enhanced properties of novel zirconia-based osteo-implant systems. Applied Materials Today 2017;9:622–632.
		專任助理			0	
	非本國籍	大專生			0	
		碩士生			0	
		博士生			0	
		博士後研究員			0	
		專任助理			0	
其他成果 （無法以量化表達之成果如辦理學術活動、獲得獎項、重要國際合作、研究成果國際影響力及其他協助產業技術發展之具體效益事項等，請以文字敘述填列。）						

科技部補助專題研究計畫成果自評表

請就研究內容與原計畫相符程度、達成預期目標情況、研究成果之學術或應用價值（簡要敘述成果所代表之意義、價值、影響或進一步發展之可能性）、是否適合在學術期刊發表或申請專利、主要發現（簡要敘述成果是否具有政策應用參考價值及具影響公共利益之重大發現）或其他有關價值等，作一綜合評估。

1. 請就研究內容與原計畫相符程度、達成預期目標情況作一綜合評估
   ■達成目標
   □未達成目標（請說明，以100字為限）
   　□實驗失敗
   　□因故實驗中斷
   　□其他原因
   說明：

2. 研究成果在學術期刊發表或申請專利等情形（請於其他欄註明專利及技轉之證號、合約、申請及洽談等詳細資訊）
   論文：■已發表　□未發表之文稿　□撰寫中　□無
   專利：□已獲得　□申請中　■無
   技轉：□已技轉　□洽談中　■無
   其他：（以200字為限）

3. 請依學術成就、技術創新、社會影響等方面，評估研究成果之學術或應用價值（簡要敘述成果所代表之意義、價值、影響或進一步發展之可能性，以500字為限）
   本計畫將生物活性鈣矽成分加入氧化鋯，進行長時期降解性及骨形成性評估，開發出新的ZrO2基植體。結果發現15和20 wt% CaSi的複合材料的三點彎曲強度在皮質骨彎曲強度範圍內。鈣矽含量最高的複合體，即使浸泡在人工體液1年，其重量損失僅0.4%，且強度不受浸泡時間影響，更重要地是，大大改善氧化鋯細胞增生、分化及礦化。本計畫所開發出的ZrO2基複合材料深具技術創新及臨床實用性，可應用於牙科與骨科等長期承受荷重部位，取代現有商化鈦金屬或氧化鋯植體。此氧化鋯基底新材料開發不僅具學術創新性，且可減少國內醫療器材與裝置的進口依賴，兼而提升國內醫療產品開發能力，將產品推向國際舞台。

4. 主要發現
   本研究具有政策應用參考價值：■否　□是，建議提供機關
   （勾選「是」者，請列舉建議可提供施政參考之業務主管機關）
   本研究具影響公共利益之重大發現：□否　□是
   說明：（以150字為限）
   本計畫乃開發新氧化鋯基複合植體，應用於牙科與骨科等長期承受荷重部位修補。計畫內容是分析開發出的骨植體材料之各項物理化學、機械與生物性，以凸顯本材料臨床應用的可行性，因此成果不影響公共利益。